JAERI-M
89-179

ANALYTICAL STUDY FOR PHEBUS EXPERIMENT 215R BY FRAP-T4 CALCULATION CODE

November 1989

Kazuichiro HASHIMOTO

日本原子力研究所
Japan Atomic Energy Research Institute

編集兼発行　日本原子力研究所
印　　刷　いばらき印刷㈱

Analytical Study for PHEBUS Experiment 215R by FRAP-T4 Calculation Code

Kazuichiro HASHIMOTO

Department of Fuel Safety Research
Tokai Research Establishment
Japan Atomic Energy Research Institute
Tokai-mura, Naka-gun, Ibaraki-ken

(Received October 11, 1989)

The PHEBUS program at the Cadarache Nuclear Research Center in France was performed to investigate fuel behavior under conditions of a loss-of-coolant accident (LOCA) of a PWR. The program consisted of four phases. Phase I included three experiments with the single rod and sixteen experiments with the 25-rod bundle. Purpose of the Phase I experiments was to clarify thermalhydraulic condition of the PHEBUS loop. Phase II experiments were performed with the 25-rod bundle to obtain data on fuel behavior during a large break LOCA. Phases III and IV were devoted to severe fuel damage research.

A sensitivity study using the data of the experiment 215R has been made with the calculation code FRAP-T4. A gap size between the fuel pellet and the cladding, and a thickness of the cladding were considered as the parameters in this study to investigate how they affect to fuel behavior during a LOCA condition.

Keywords: LOCA, PHEBUS, Cladding, Blowdown, Rupture, Gap, Pellet, FRAP-T4

FRAP－T4コードによるPHEBUS実験 215R感度解析

日本原子力研究所東海研究所燃料安全工学部
橋本和一郎

（1989年10月11日受理）

仏CEAのカダラッシュ研究所では，PWRの大破断冷却材喪失事故（LOCA）時における燃料挙動を研究するためPHEBUS計画を実施した。同計画は全体で4つのフェーズに分れている。フェーズ1では，単一燃料棒実験3回と25本燃料棒実験16回が実施された。フェーズⅠの実験は，PHEBUS実験ループの熱水力状態を把握するために実施された。フェーズⅡでは，25本燃料棒バンドルを用いて大破断冷却材喪失事故時の燃料挙動を調べる実験が行われた。フェーズⅢ，及びフェーズⅣでは，炉心損傷事故を模擬した実験が行われた。

PHEBUS実験215Rのデータに基づき，FRAP－T4コードによる感度解析を行った。解析パラメータとして燃料ペレット－被覆管ギャップ幅，燃料被覆管厚さを選び，これらがLOCA時の燃料挙動に如何に影響するかを調べた。

東海研究所：〒319－11　茨城県那珂郡東海村白方字白根2－4

Contents

目　　次

1. Introduction

The PHEBUS program[1, 2] started in 1974 and the first test was conducted in 1977. The program consisted of four phases; Phase I experiments were performed by using single fuel rod or 25 fuel rods in order to investigate thermalhydraulic conditions in the test loop and to determine operational procedures to simulate a LOCA condition, Phase II experiments were performed to investigate PWR fuel behavior under a large break LOCA condition, Phases III and IV were devoted to severe fuel damage research.

The experiment 215R was carried out in May 1983 as the last experiment in Phase I of PHEBUS program. This experiment was performed satisfactorily for the purpose of Phase I; the cladding surface temperature profile agreed well with the precalculation by RELAP4-MOD6. Phase II started in December 1983 with the experimental conditions obtained in the phase I test series.

In the PHEBUS program, FRAP-T4[3, 4] and CUPIDON, a French code, were employed to analyze the fuel behavior under a LOCA condition. The CUPIDON code was developed specifically for the analysis of PHEBUS experiments. It is a two-dimensional code and deals with thermal and mechanical behavior of fuel rods as an oxidation of an external surface of cladding. However the use of the code is limited to a single non-irradiated fuel rod with short length such as the PHEBUS rods. On the other hand, the FRAP-T4 code can be used to analyze a full length fuel during a LOCA or PCM (power-cooling-mismatch). FRAP-T4 is coupled to the MATPRO code, a material property code, which provides material properties to the FRAP-T4 subcodes.

FRAP-T4 code was used for the post test analysis of the PHEBUS experiment 215R. In the analysis the geometrical effect of fuel rod was investigated. The objective of this paper is to discuss the analysis on the geometrical effect of a fuel rod on fuel behavior under a LOCA condition.

2. Description of the PHEBUS Experiment 215R

2.1 Test Facility

The main loop of the PHEBUS facility is shown in Fig. 1. The loop consists of a driver core in a swimming pool, a test loop, an emergency injection system, and measurement system. The maximum power of the driver core is 60 MW, and it is cooled by the water from the 500 m^3 cold water tank. The test loop is composed of two parts: the in-pile experimental cell containing a test train which is positioned at the center of the driver core, and out-of-pile facilities which include a cold leg, a hot leg, a blowdown tank, a recirculation pump, a heat exchanger, a reheater, and a pressure regulation valve. A test train which contains test fuel is set in the experimental cell, and it is changed at each experiment. The test fuel is of the 17x17 PWR type. The enrichment in the 25 fuel bundle is 2.6% for the sixteen outer rods and 3.5% for the nine inner rods. For the single rod test, the enrichment is 20%. Tables 1 and 2 show the major characteristics of test loop and the characteristics of test fuel, respectively. The measurement system includes about 150 sensors for pressure, temperature, power level and flow rate. Two-phase flow measurement is made by comparing the data from a turbine flow meter, a venturi, and a gamma densitometer. These three types of instruments are installed at the hot leg and the cold leg. Temperature measurements are made at fluid, structures, claddings, and pellets.

2.2 Experiment Procedure

The experiment starts with reproducing the normal PWR operating condition in the test loop: pressure of 15.5 MPa, fluid temperature of 320°C, fluid velocity at the fuel rod of 5m/s. This condition continues during the initial 10 min. Then the fluid in the test loop is separated by closing the valves (VA-EP-04 and VA-EP-02 in Fig. 1). Immediately after the valve closure, a quick opening valve in the blowdown tank is opened to simulate a main pipe break. The motion of the control rods can produce the power in the test fuel which simulates a residual power at shutdown in an actual reactor. The blowdown can be made either at hot leg, at cold leg or at the both of them. The break size can also be changed. The major characteristics of the experiment 215R are summarized in Table 3.

3. Calculation Model and Inputs for FRAP-T4

Post test calculations were made for the PHEBUS experiment 215R using FRAP-T4 in order to investigate the geometrical effect of fuel rod on the overall fuel behavior during a LOCA. The following parameters were considered in the present analysis.

(1) Gap size between the fuel pellet and cladding
(2) Thickness of the cladding

These parameters were chosen considering that these parameters have a large effect on cladding deformation behavior under LOCA condition. The analytical models employed in all the calculations are listed in Table 4.

All the calculations were made based on the data of fuel rod No. 6 which was located peripheral part in the 25 rod bundle and pressurized at 5.0 bar before the starting of the experiment. In the present calculations the fuel rod is divided into six axial nodes and thirteen radial nodes.

Table 5 shows the parametrical values for the two types of calculations comparing with the standard case data. The calculations of the Cases 1 and 2 were made with changing the gap size between the fuel pellet and cladding in order to study the effect of gap heat transfer on the fuel temperature. In the Cases 3 and 4, the thickness of cladding was changed to study the thermal as well as mechanical effect of the cladding.

a quick opening valve in the blowdown tank is opened to simulate a main pipe break. The motion of the control rods can produce the power in the test fuel which simulates a residual power at shutdown in an actual reactor. The blowdown can be made either at hot leg, at cold leg or at the both of them. The break size can also be changed. The major characteristics of the experiment 215R are summarized in Table 3.

3. Calculation Model and Inputs for FRAP-T4

Post test calculations were made for the PHEBUS experiment 215R using FRAP-T4 in order to investigate the geometrical effect of fuel rod on the overall fuel behavior during a LOCA. The following parameters were considered in the present analysis.

(1) Gap size between the fuel pellet and cladding

(2) Thickness of the cladding

These parameters were chosen considering that these parameters have a large effect on cladding deformation behavior under LOCA condition. The analytical models employed in all the calculations are listed in Table 4.

All the calculations were made based on the data of fuel rod No. 6 which was located peripheral part in the 25 rod bundle and pressurized at 5.0 bar before the starting of the experiment. In the present calculations the fuel rod is divided into six axial nodes and thirteen radial nodes.

Table 5 shows the parametrical values for the two types of calculations comparing with the standard case data. The calculations of the Cases 1 and 2 were made with changing the gap size between the fuel pellet and cladding in order to study the effect of gap heat transfer on the fuel temperature. In the Cases 3 and 4, the thickness of cladding was changed to study the thermal as well as mechanical effect of the cladding.

4. Calculated Results and Discussions

First of all, the calculated fuel temperature is compared with the measured one to verify the FRAP-T4 model. Then the calculated displacement of fuel stack is presented in comparison with the fuel temperature. Concerning the behavior of cladding, the extent of deformation and the timing of rupture are discussed in comparison with the actual data. In the last section, the thermal conductivity between the pellet and the cladding is discussed to consider the effect of internal pressure of the rod on the fuel temperature.

4.1 Fuel Temperature

Figure 2 presents measured temperatures at the fuel centerline and at the cladding surface at the midplane of the test section. In this figure and in the following figures the blowdown starts at 2 sec. Figure 3 shows the calculated temperatures of the fuel centerline, fuel surface and cladding surface at the third axial node in the standard case. The third node is positioned in the middle of the fuel stack. The measured cladding surface temperatures were used as the input to the calculations as the boundary conditions. The fuel centerline temperatures in the experiment and the calculation are compared in Fig. 4. The calculated temperature starts with somewhat lower value than the measured one but it agrees well with the measured one during the transient.

Figures 5 and 6 show the profiles of fuel centerline temperature for Cases 1 and 2, and Cases 3 and 4, respectively, with comparing the standard case. The centerline temperature has higher value in the Case 1 than in the standard case because the heat transfer from the pellet to the cladding is lower in the Case 1 than in the standard case due to wide gap between the pellet and the cladding. This relation is based on the Ross and Stoute model of a gas-gap heat transfer. With this model the gap conductance h_g can be expressed as follows in an open gap case.

$$h_g = \frac{K_g}{t_g + (g_1 + g_2) + 1.98\,(R_f + R_c)} + h_r$$

where,

K_g: conductivity of gas in gas gap
t_g: gap thickness
g_1: temperature jump distance at cladding internal surface
g_2: temperature jump distance at fuel external surface
h_r: radiant heat transfer conductance
R_c: arithmetic mean roughness height of cladding
R_f: arithmetic mean roughness height of fuel

In the above equation the radiant heat transfer conductance h_r is a function of temperature of external surface of fuel, temperature of internal surface of cladding, and emissivity factor.

As shown in Fig. 6, the thickness of cladding has less effect on the fuel centerline temperature as compared with the size of gap. In either case of 1 to 4, the temperature difference between each calculation exists until around 40 sec. This means that the difference in gap size or thickness of cladding could affect fuel temperature during the initial transient phase only.

4.2 Displacement of Fuel Stack

The displacement of fuel stack which is shown in Figs. 7 and 8 in Cases 1 to 4 has a similar tendency with the fuel centerline temperature in Figs. 5 and 6. The reason is that the displacement of fuel stack mainly depends on the temperature of fuel.

4.3 Deformation and Rupture of Cladding

Figures 9 and 10 show the circumferential deformation of cladding in Cases 1 to 4 comparing with the standard case. In Fig. 9, only a slight difference can be observed in the three profiles. This indicates that the gap size between fuel pellet and cladding has small influence on the geometrical deformation of cladding. On the other hand, the thickness of cladding is an important factor for mechanical toughness of cladding as can be seen in Fig. 10. In these cases, a rupture of cladding occurred at the midplane for Case 4 (thin cladding) at 48 sec after the starting of blowdown, while a rupture occurred at 68 sec in the standard case. The circumferential deformation at the rupture was higher in the standard case than in Case 4. The rupture time in each case is shown in Table 6 with each circumferential deformation at rupture. This table reveals that a gap size has less effect on a deformation of cladding than thickness of cladding. In the experiment the rupture of No. 6 rod occurred but the time of rupture was unknown because no pressure sensor was installed in this rod. The post test examination shows that the No. 6 rod ruptured without any deformation at the point where a thermocouple was embedded to the cladding surface. From the fact that there was no deformation at the rupture point of the rod in the experiment, it can be presumed that the actual rupture time was earlier than the calculated rupture time in the standard case, in that the deformation of the rod gradually occurred until the time of rupture.

4.4 Thermal Conductivity between Pellet and Cladding

In order to clarify the effect of an initial pressure in fuel rod on thermal conductivity between fuel pellets and cladding, additional calculations were done with various initial pressures and various gap sizes. Figure 11 shows the fuel centerline temperature against the initial pressure in fuel rod with various gap sizes. This figure reveals that the fuel centerline temperature at steady state depends strongly on the gap size, while the temperature has only a week dependency on the initial pressure in fuel rod. Therefore the fuel temperature of pressurized and unpressurized rods will be nearly the same at the beginning of the transient.

5. Conclusions

An analytical study was performed for the PHEBUS experiment 215R by FRAP-T4 code. In this study, the FRAP-T4 was verified by comparing the calculated fuel temperature with the measured one. The parameters considered in the sensitivity study include gap size between fuel pellet and cladding, thickness of cladding, and internal pressure of fuel rod. The gap size between fuel pellet and cladding has a large effect on the temperature in pellets at steady state and blowdown phase. The thickness of cladding is an important factor for the ballooning of cladding and also for the time of rupture. The internal pressure in a fuel rod has only a small effect on fuel temperature at steady state.

initial pressure in fuel rod. Therefore the fuel temperature of pressurized and unpressurized rods will be nearly the same at the beginning of the transient.

5. Conclusions

An analytical study was performed for the PHEBUS experiment 215R by FRAP-T4 code. In this study, the FRAP-T4 was verified by comparing the calculated fuel temperature with the measured one. The parameters considered in the sensitivity study include gap size between fuel pellet and cladding, thickness of cladding, and internal pressure of fuel rod. The gap size between fuel pellet and cladding has a large effect on the temperature in pellets at steady state and blowdown phase. The thickness of cladding is an important factor for the ballooning of cladding and also for the time of rupture. The internal pressure in a fuel rod has only a small effect on fuel temperature at steady state.

Acknowledgment

The author wishes to thank Mrs. M. Berne, Mr. E. Scott de Martinville, and Dr. P. Berna for invaluable discussions during performing this work, and also thanks to the PHEBUS analytical and experimental group for their kind assistances. The author also expresses his appreciation to Dr. K. Soda for reviewing the manuscript.

This work was carried out at the Cadarache Nuclear Research Center, France, in the framework of the NSRR-PHEBUS collaboration program.

References

1) Manim, A., Del Negro, R. and Reocreux, M.: CEA-CONF 5437(1980).
2) Del Negro, R., Reocreux, M., Pelce, J., Legrand, B. and Berna, P.: NUREG/CP 0027 Vol. 3 (1983).
3) Sdouz, G.: SGAE 3052. RS 154/79. (1979).
4) Charyulu, M. K.: EGG-TFBP 5010 (1979).

Acknowledgment

The author wishes to thank Mrs. M. Berne, Mr. E. Scott de Martinville, and Dr. P. Berna for invaluable discussions during performing this work, and also thanks to the PHEBUS analytical and experimental group for their kind assistances. The author also expresses his appreciation to Dr. K. Soda for reviewing the manuscript.

This work was carried out at the Cadarache Nuclear Research Center, France, in the framework of the NSRR-PHEBUS collaboration program.

References

1) Manim, A., Del Negro, R. and Reocreux, M.: CEA-CONF 5437(1980).
2) Del Negro, R., Reocreux, M., Pelce, J., Legrand, B. and Berna, P.: NUREG/CP 0027 Vol. 3 (1983).
3) Sdouz, G.: SGAE 3052. RS 154/79. (1979).
4) Charyulu, M. K.: EGG-TFBP 5010 (1979).

Table 1 Major characteristics of the test loop

TEST LOOP	
Coolant	Demineralized degassed water
Blanket gas	Nitrogen
Maximum flow rate	25 x 10^{-3} $m^3 . s^{-1}$
Maximum temperature in steady state	330°C
Maximum pressure	17 MPa
Isolation valves switching time	0.20 s
Time for complete opening of blow-down valves	0.06 s
EP INJECTION PUMP	
Flow rate	15 to 400 liters/h
Pressure	17 MPa
Maximum temperature	70 °C
RECIRCULATION PUMP	
Flow rate	5000 Liters/h
Temperature	20 to 170 °C
ACCUMULATORS	
Pressurization fluid	Nitrogen
Maximum pressure	16 MPa
Effective volume	0.2 M^3
IN-PILE CELL	
Inner diameter	124 mm
TEST TRAIN	
Outer diameter	114.3 mm

Table 2 Characteristics of the test fuel

RODS	
Overall length	1073.5 mm
Fissile length	800 mm
Cladding material	Zircaloy 4
Cladding inner diameter	8.36 mm
Cladding thickness	0.60 mm
Pellets diameter	8.19 mm
Oxide relative density	0.94
Filling gas	Helium
25 ROD BUNDLES	
Lattice pitch	12.6 x 12.6 mm
Enrichment	2.6 % - 3.5 %
SINGLE ROD TEST TRAIN	
Enrichment	20 %

Table 3 Major characteristics of the experiment 215R

Number of test fuel rods	25
Pressurized fuel rods in test fuel rods	22
Nuclear peak power during steady state	57 kW/m
Position of break for blowdown	hot leg and cold leg (delay of hot leg break)
Break size ratio (cold leg/hot leg)	1.1
Cladding failure time after break	20 s
Cladding surface temperature at failure	800°C
Cladding surface temperature at plateau	1100°C (during about 30 s)

Other characteristics

- * Realization of a hollow of the cladding surface temperature curve at t=14 s.
- * Reflooding after a plateau of cladding surface temperature.

Table 4 Analytical models employed in the calculation

Phenomena	Models
Gap gas heat transfer	Ross and Stoute model
Metal-water reaction	Cathcart cladding oxidation model
Fuel rod deformation	FRACAS-I subcode (with fuel relocation according to Coleman correlation)

Table 5 Parametrical values for each calculation

case	Gap size between the fuel pellet and cladding	Thickness of the cladding
0 (standard case)	S_g	S_c
1	Wide gap ($2 \times S_g$)	S_c
2	Narrow gap ($1/2 \times S_g$)	S_c
3	S_g	Thick cladding ($2 \times S_c$)
4	S_g	Thin cladding ($1/2 \times S_c$)

S_g : Standard gap size
S_c : Standard thickness of cladding

Table 6 Cladding rupture time and circumferential deformations in cases 0 to 4

	Rupture time after starting of blowdown (sec)	Circumferential deformation at rupture (-)
Case 0 (standard case)	68	0.0670
Case 1 (Wide gap)	66	0.0665
Case 2 (Narrow gap)	76	0.0731
Case 3 (Thick cladding)	no rupture	-----
Case 4 (Thin cladding)	48	0.0446

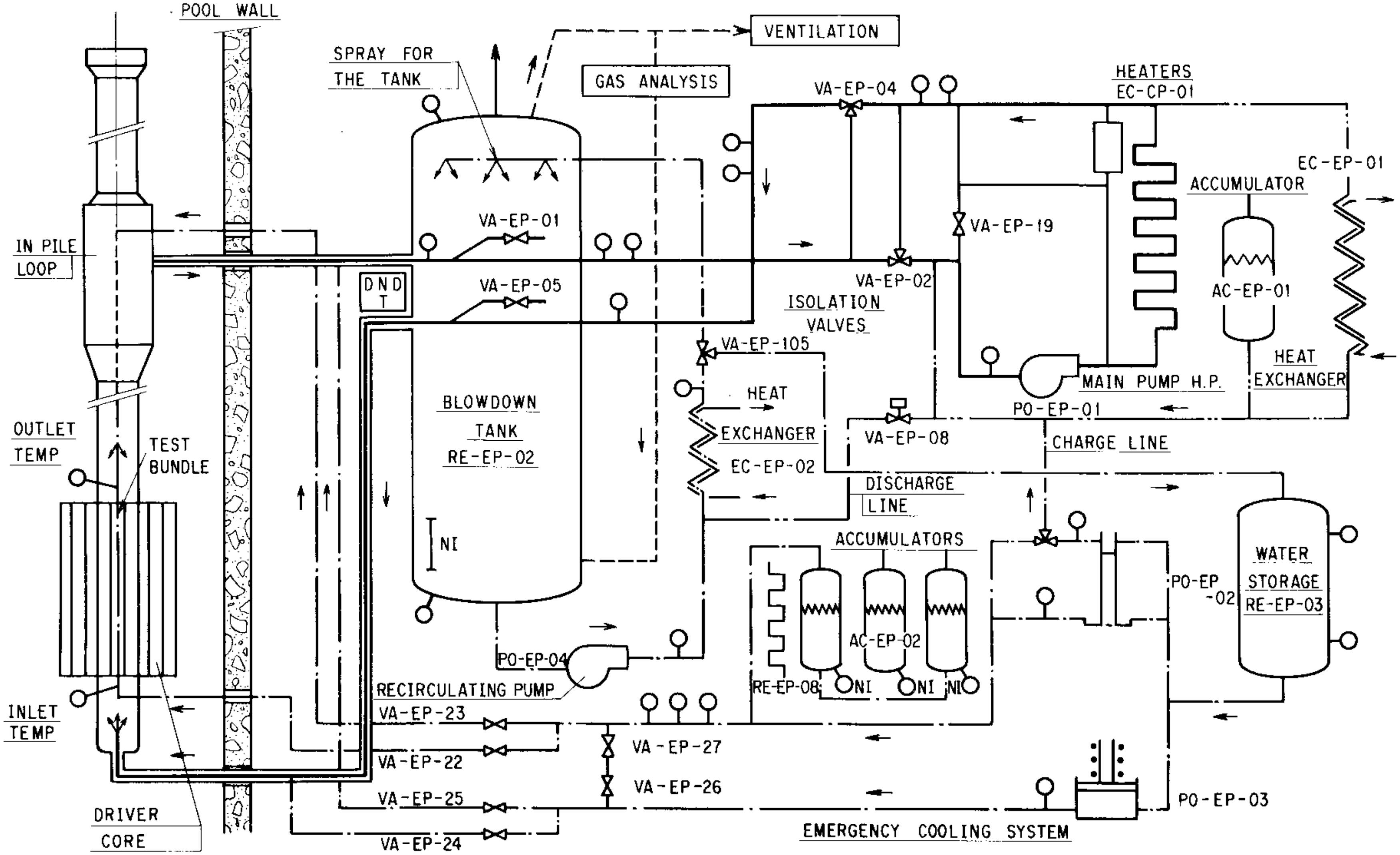

Fig. 1 PHEBUS test loop circuits diagram

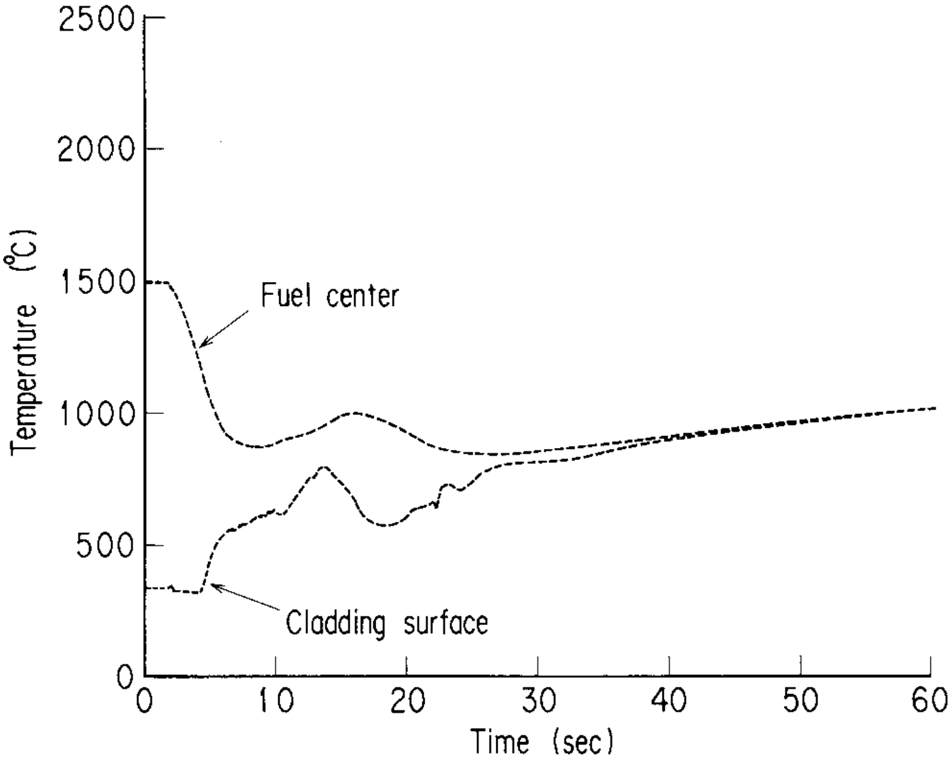

Fig. 2 Fuel center and cladding surface temperature profiles (experimental results)

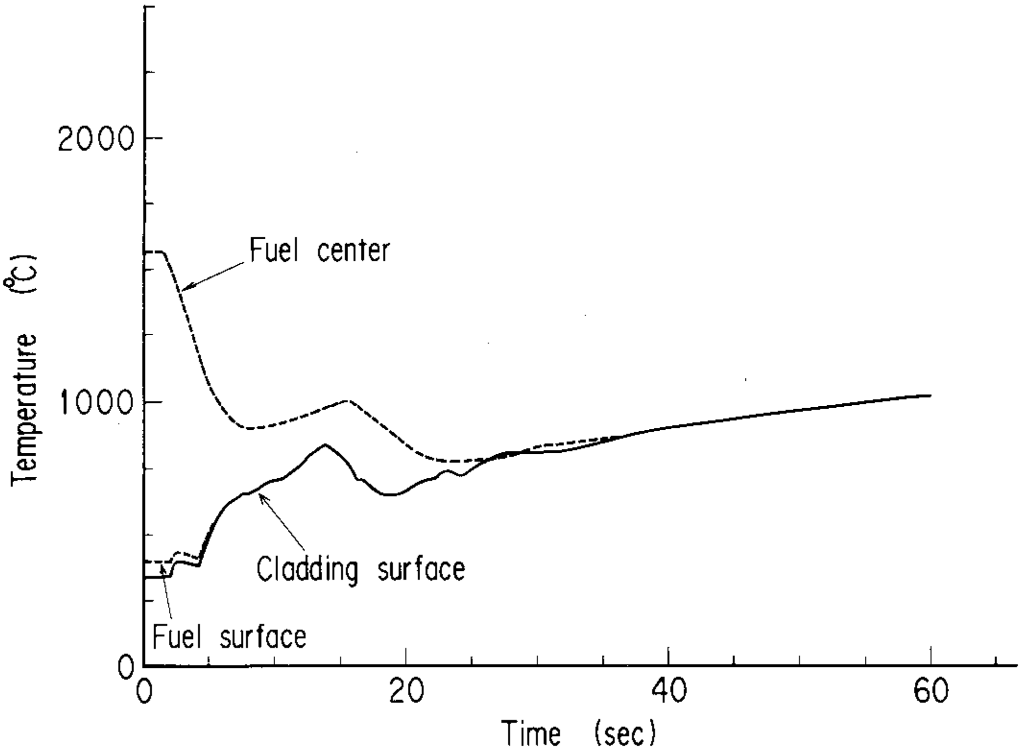

Fig. 3 Fuel center, fuel surface and cladding surface temperture profiles (calculated results)

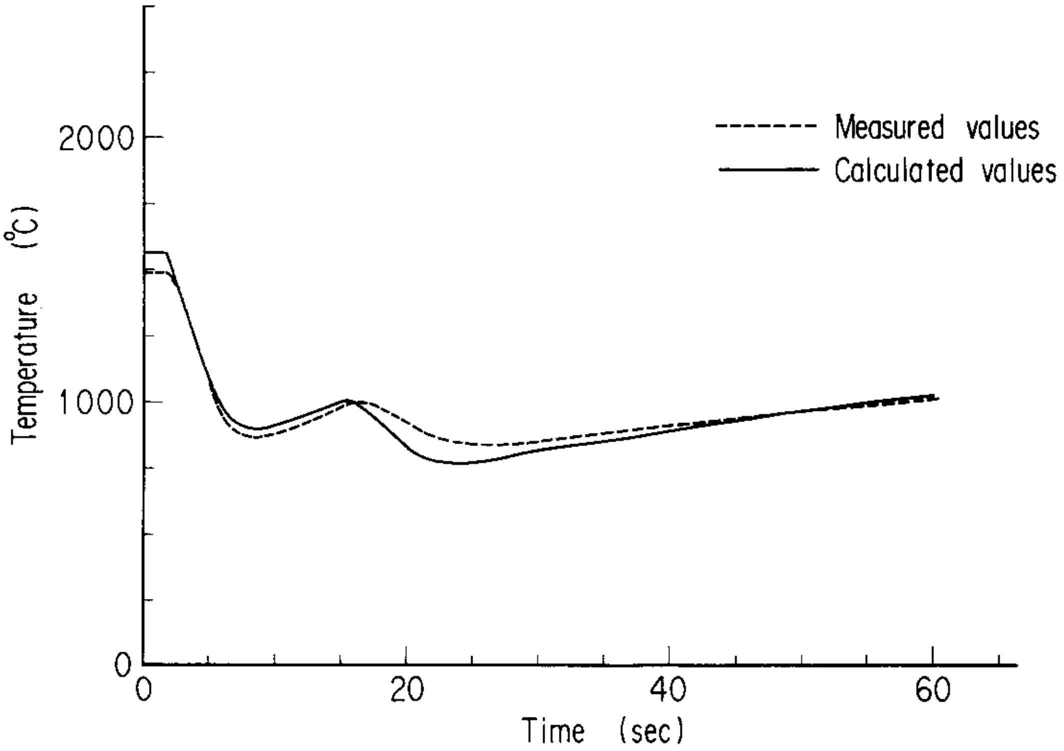

Fig. 4　Profiles of fuel centerline temperatues

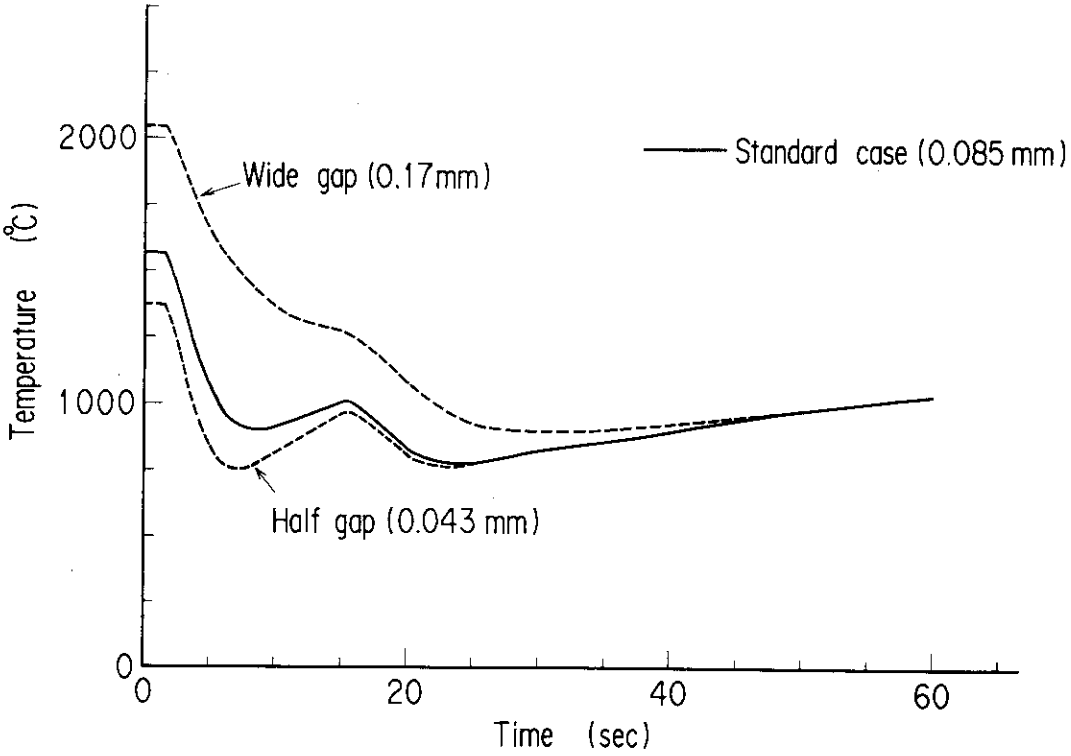

Fig. 5　Profiles of fuel centerline temperature (Cases 1 and 2)

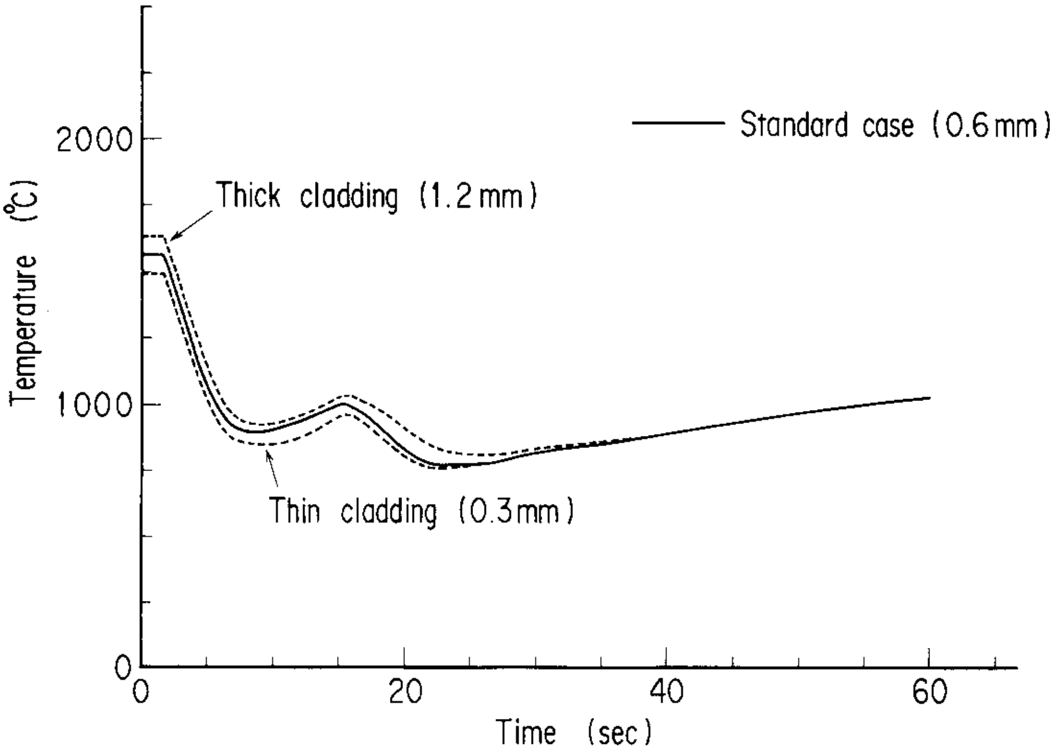

Fig. 6 Profiles of fuel centerline temperatures (Cases 3 and 4)

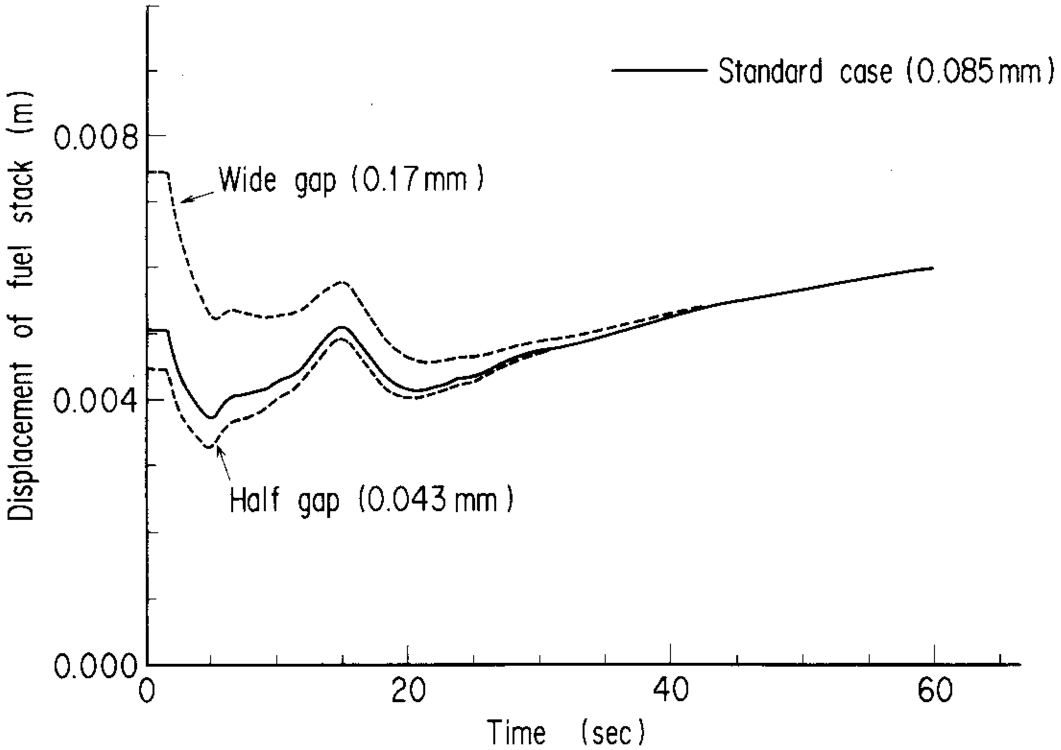

Fig. 7 Profiles of displacement of fuel stack (Cases 3 and 4)

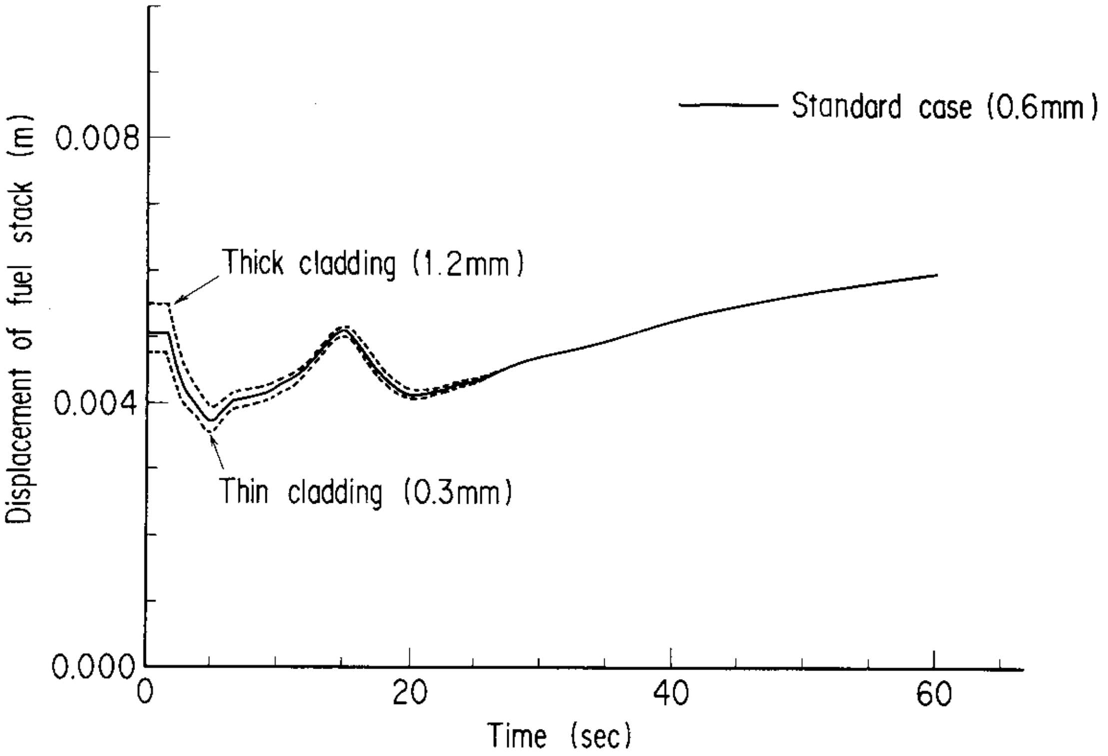

Fig. 8 Profiles of displacement of fuel stack (Cases 3 and 4)

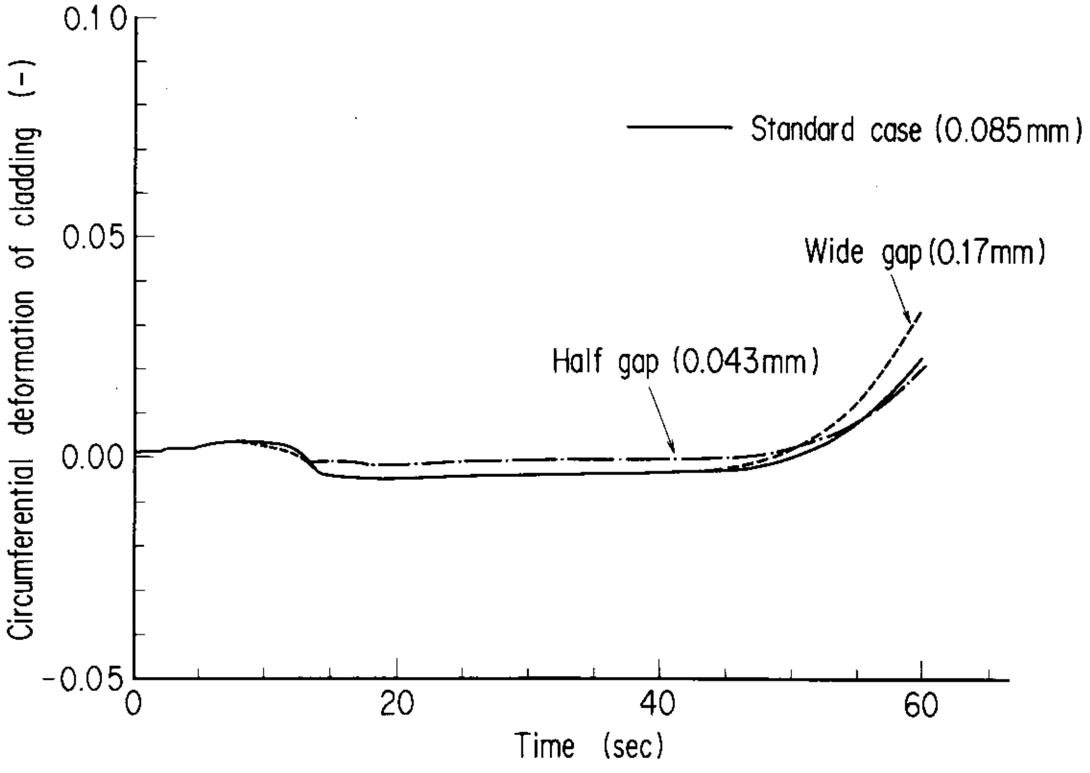

Fig. 9 Profiles of circumferential deformations of cladding (Cases 1 and 2)

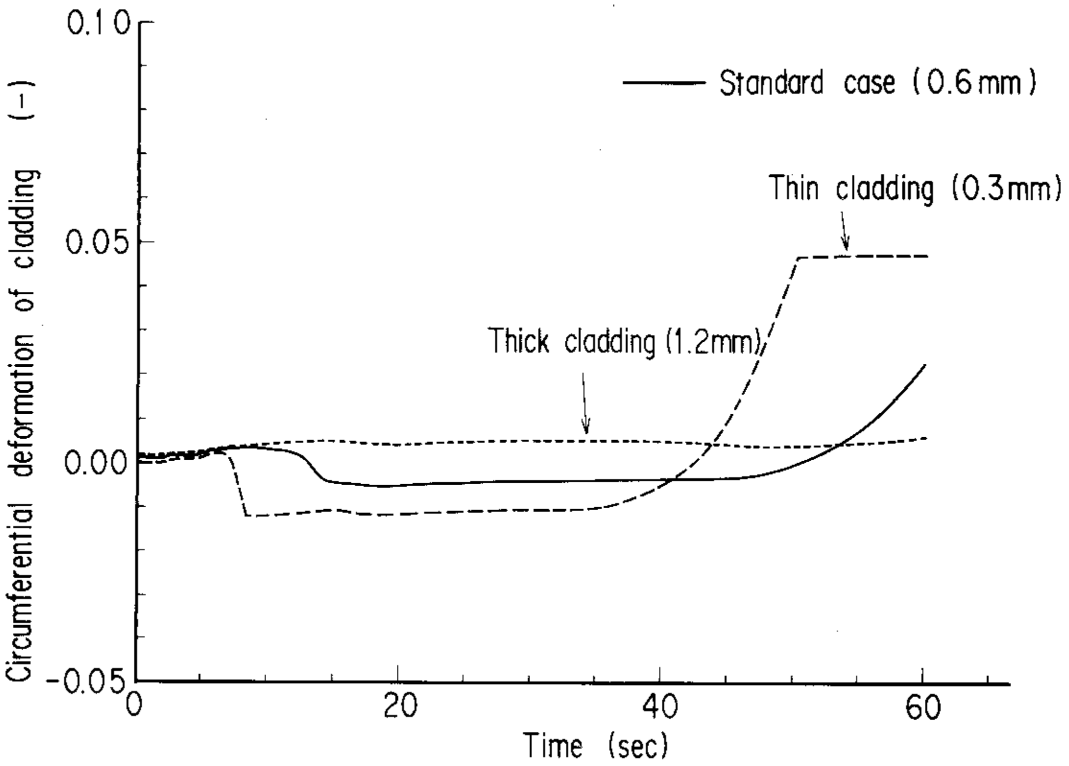

Fig. 10 Profiles of circumferential deformations of cladding (Cases 3 and 4)

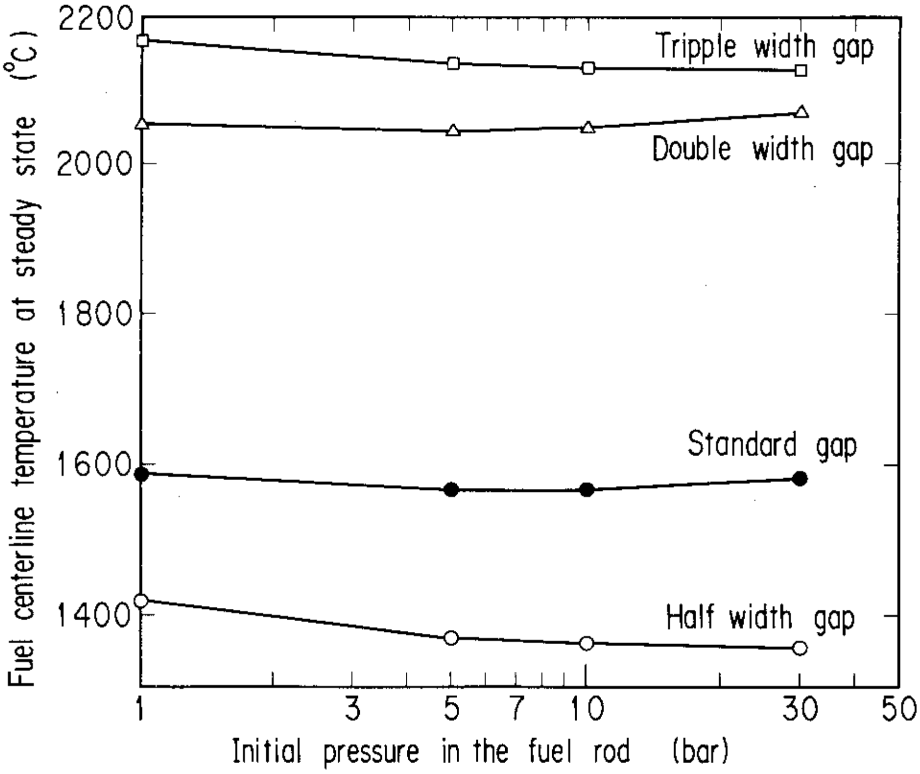

Fig. 11 Effect of gap size and internal rod pressure on fuel temperature